Available online at www.sciencedirect.com
ScienceDirect
Ultrasonics 45 (2006) 32–39
Ultrasonics
www.elsevier.com/locate/ultras

Ultrasonic polar scans: Numerical simulation on generally anisotropic media

Nico F. Declercq [a,b,*], Joris Degrieck [c], Oswald Leroy [d]

[a] George W. Woodruff School of Mechanical Engineering, Georgia Institute of Technology, 801 Ferst Drive, Atlanta, GA 30332-0405, USA
[b] Georgia Tech Lorraine 2 rue Marconi, 57070 Metz, France
[c] Department of Mechanical Construction and Production, Ghent University, Sint Pietersnieuwstraat 41, 9000 Gent, Belgium
[d] Interdisciplinary Research Center, Katholieke Universiteit Leuven Campus Kortrijk, E. Sabbelaan 53, 8500 Kortrijk, Belgium

Received 14 July 2005; received in revised form 13 May 2006; accepted 30 May 2006
Available online 22 June 2006

Abstract

Ultrasonic polar scans are based on the recording of the reflected or transmitted amplitude of sound, impinging a fiber reinforced composite from every possible angle of incidence. The mechanical anisotropy of such materials makes the reflection coefficient direction dependent, whence an ultrasonic polar scan forms a fingerprint of the investigated material. Such scans have already proved to be very valuable in the characterization of composites. Simulations have been performed for single layered and multi-layered systems, for pulsed and harmonic waves. Fiber reinforced composites are mostly orthotropic. The current report presents simulations not only on orthotropic materials but on materials of any kind of anisotropy. These extended numerical simulations are not only valuable in the characterization of highly sophisticated composites, but may also be used to characterize thin slices of crystals and even layered crystals.

Keywords: Ultrasonic polar scans; Crystals; Anisotropy

1. Introduction

The application of ultrasonic techniques in nondestructive testing and the characterization of materials, is widely accepted, the oldest of which is the classical C-scan to detect and localize certain defects. Even though the classical C-scan has proved to be well suited for the task of detecting defects, an extension to more sophisticated means of measurements is necessary especially if the characterization of stiffness is requested. On fiber reinforced composite plates and crystals, this can only be performed if oblique incidence is considered as well.

An 'ultrasonic polar scan' is performed on a sample immersed in water and investigates anisotropic mechanical features of the laminate exploiting its influence on obliquely incident sound. The ultrasonic polar scan is an investigation of the amplitude of transmitted (or if necessary reflected) sound, which results from sound impinging the upper surface of the sample from every direction and is relatively simple to measure.

Because a polar scan registers sound amplitudes on a small spot, it actually represents a local fingerprint of the plate under investigation. The characteristic pattern of such a 'fingerprint' consists in fact of a collection of areas, showing considerably less intensity than elsewhere on the registered polar scan. These areas are physically connected [1] to generated critical waves in the sample, such as leaky Rayleigh waves, leaky Lamb waves or even lateral waves [2–14]. Hence, they almost directly clarify the mechanical anisotropy and the stiffness of the investigated spot.

* Corresponding author. Present address: George W. Woodruff School of Mechanical Engineering, Georgia Institute of Technology, 801 Ferst Drive, Atlanta, GA 30332-0405, USA.
E-mail addresses: nico.declercq@me.gatech.edu, declercq@ieee.org (N.F. Declercq).

0041-624X/$ - see front matter © 2006 Elsevier B.V. All rights reserved.
doi:10.1016/j.ultras.2006.05.219

It has been shown before [15–20] that the 'ultrasonic polar scan' is a highly recommended and convenient technique for the characterization of the fiber direction, the orthotropic stiffness, and for the extraction of information about porosity, resin fraction, etcetera in fiber reinforced composites.

Because fatigue damage induces stiffness reduction, it has been shown that polar scans are also excellent tools to monitor fatigue damage [21].

The present paper focuses on the theoretical modeling of ultrasonic polar scans on materials of any possible type of anisotropy. The numerical method outlined below, is based on the so called direct method. By 'direct method', we mean that one global continuity matrix is constructed that relates the sound amplitudes in each layer to the incident sound amplitude. Therefore the matrix dimensions are proportional to the number of layers. For a large number of layers, matrix inversion becomes therefore rather cumbersome, though this problem is highly reduced by application of a fast computer. Sophisticated techniques [22,23] in order to reduce the dimensions of this matrix are therefore not applied in the current paper.

The technique is deterministic and is not built on the Floquet wave principle [24] for periodically layered systems.

2. The effect of anisotropy on elasticity

In what follows, we apply the double suffix notation convention of Einstein. The dynamics of an anisotropic material is described [25] by

$$\frac{\partial \sigma_{ij}}{\partial r_j} = \rho \frac{\partial^2 u_i}{\partial t^2} \tag{1}$$

while the generalized Hooke's law, taking into account symmetry properties which are due to the analytical feature of the strain energy and the symmetric nature of the stress and strain tensors, is given by

$$\begin{bmatrix} \sigma_{11} \\ \sigma_{22} \\ \sigma_{33} \\ \sigma_{23} \\ \sigma_{13} \\ \sigma_{12} \end{bmatrix} = \begin{bmatrix} C_{11} & C_{12} & C_{13} & C_{14} & C_{15} & C_{16} \\ C_{12} & C_{22} & C_{23} & C_{24} & C_{25} & C_{26} \\ C_{13} & C_{23} & C_{33} & C_{34} & C_{35} & C_{36} \\ C_{14} & C_{24} & C_{34} & C_{44} & C_{45} & C_{46} \\ C_{15} & C_{25} & C_{35} & C_{45} & C_{55} & C_{56} \\ C_{16} & C_{26} & C_{36} & C_{46} & C_{56} & C_{66} \end{bmatrix} \begin{bmatrix} e_{11} \\ e_{22} \\ e_{33} \\ 2e_{23} \\ 2e_{13} \\ 2e_{12} \end{bmatrix} \tag{2}$$

in which σ_{ij} is the stress tensor, e_{ij} is the deformation tensor, whereas C_{ij} is the stiffness tensor.

3. The propagation of bulk plane waves

We represent the acoustic field inside and outside the composite as a superposition of all possible bulk modes given an incident bulk wave [26,27]. Therefore we are mainly interested in a resulting field and do not attempt to study sound rays and point sources in a composite [28,29]. The reverse Voigt procedure transforms the stiffness tensor C_{mn} of rank 2 to the stiffness tensor c_{ijkl} of rank 4 as $(1 \to 11)$, $(2 \to 22)$, $(3 \to 33)$, $(4 \to 23 = 32)$, $(5 \to 13 = 31)$ and $(6 \to 12 = 21)$. When necessary, the intrinsic stiffness constants $c_{ijkl} = c^I_{ijkl}$ can be transformed into stiffness constants $c_{ijkl} = c^Q_{ijkl}$ in coordinates corresponding to a rotated (laboratory) system as follows:

$$c^Q_{ijkl} = Q_{im} Q_{jn} Q_{kp} Q_{lq} c^I_{mnpq} \tag{3}$$

where Q_{ij} are the entries of the rotation matrix for a rotation from the intrinsic lattice coordinate system to the laboratory coordinate system. Eq. (1) then becomes

$$\rho \frac{\partial^2 u_i}{\partial t^2} = c_{ijkl} \frac{\partial^2 u_l}{\partial x_j \partial x_k} \tag{4}$$

A plane wave solution of Eq. (4) is of the form

$$u_i = U_i \exp i(n_j r_j - \omega t) \tag{5}$$

where $\boldsymbol{n}$ is the wave vector. If this is entered in Eq. (4), straightforward calculations then result in

$$\left(\frac{1}{\rho} c_{ijkl} n_k n_j - \omega^2 \delta_{il} \right) U_l = 0 \tag{6}$$

The latter equation is called the Christoffel equation [25,30–33]. It relates the slowness n/ω and the polarization $\boldsymbol{U}$ to the propagation direction and is solved by demanding nontrivial solutions, followed by the determination of the corresponding eigenvectors.

4. The scattering of plane waves

4.1. Snell's law

If sound inside the bulk of the composite laminate results from impinging plane waves (denoted by superscript 'inc'), Snell's law must be taken into account which, for interfaces perpendicular to n_3, states that

$$n_1 = n_1^{\text{inc}} \text{ and } n_2 = n_2^{\text{inc}} \tag{7}$$

Then, requiring nontrivial solutions, Eq. (6) leads to a sixth degree polynomial equation of the form

$$n_3^6 + B_5 n_3^5 + A_4 n_3^4 + B_3 n_3^3 + A_2 n_3^2 + B_1 n_3 + A_0 = 0 \tag{8}$$

4.2. Continuity of normal stress and displacement

For a plate immersed in water, two different continuity conditions are involved. The water/solid interface is determined by continuity of normal stress and normal displacement, therefore along the interface,

$$u_3^{\text{water}} = u_3^{\text{solid}} \tag{9}$$

and

$$\sigma_{i3}^{\text{water}} = \sigma_{i3}^{\text{solid}}, \quad i = 1, 2, 3 \tag{10}$$

It is implicitly understood that water does not carry shear waves and therefore Eq. (10) does involve $\sigma_{13}^{\text{solid}} = \sigma_{23}^{\text{solid}} = 0$ along the water/solid interface. This is automatically taken into account by expressing the sound field in water in terms of the acoustic potential $\varphi = A\exp i(n_j r_j - \omega t)$ with the particle displacement written as $\boldsymbol{u} = \text{grad}\varphi$ [36].

The solid/solid interface (s) are determined by the continuity of the displacement vector and continuity of normal stress, hence along the interface(s)

$$u_i^{\text{solid}} = u_i^{\text{solid}}, \quad i = 1,2,3 \tag{11}$$

and

$$\sigma_{i3}^{\text{solid}} = \sigma_{i3}^{\text{solid}}, \quad i = 1,2,3 \tag{12}$$

By taking into account the appropriate continuity conditions and by applying the discussion of the previous subsection, one is able to simulate a polar scan by building the continuity matrix and extract the amplitudes for the different bulk wave components in the composite and in the surrounding liquid. The procedure that we have developed, automatically builds the complete continuity matrix no matter how many layers are involved. Furthermore, we consider the laminate as it is and do not use any simplification based on periodicity of the layers [24,34].

5. The principle of a polar scan

A classical C-scan is formed by registering the reflected or transmitted signal in many spots on the laminate surface, by applying normal incidence. Most often, C-scans are used to detect material defects and eventually to find out the 3D locations of such defects. Lately, some attempts have been undertaken to unveil the fiber direction by means of C-scans. However, the reported methods can only be used if sufficient microscopic material defects exist on the fiber/matrix interface or if the fibers are not equally distributed within the matrix.

A polar scan differs from a classical C-scan in that the transducer is not constantly held perpendicular to the interface. On the contrary, a polar scan exploits oblique incidence and measures the reflected or transmitted specular sound resulting from sound that is subsequently incident from all possible directions from above the plate. As is seen in Fig. 1, the incidence direction is defined by (θ,φ).

The reflected/transmitted amplitude is then registered in a polar diagram where each spot corresponds to a certain $(\theta + \pi,\varphi)$ and represents the amplitude for that direction. The radius in the registrations corresponds to φ, whereas the polar angle denotes θ. The grey scale is a measure for the received amplitude. Physically, the process of sound impinging the plate and traveling inside the plate, being scattered once and again by the different interfaces, is a very complicated phenomenon [28,29].

However, a 'standing wave pattern (for the particle displacement as a function of the depth)' is formed inside the plate, which is modeled by demanding only 6 modes (the 6 coming from the Christoffel Eq. (6)) propagating in each layer. This standing wave pattern may result in some kind of an eigen-vibration of the plate. If this occurs, this pattern may be due to a quasi Lamb wave or a quasi interface wave. It is characterized by a reflection/transmission coefficient tending to zero. This results in 'dark regions' in the registered polar scan. The term 'quasi' is used in anisotropic materials and denotes the fact that these waves are a generalized form of Lamb waves or interface waves that do exist in isotropic materials. Only along symmetry axes, the term 'quasi' could be replaced by 'pure'. A similar expression is later on used for 'quasi longitudinal' and 'quasi shear' waves. The quasi polarization only corresponds to a pure polarization as in isotropic materials, along axes of symmetry.

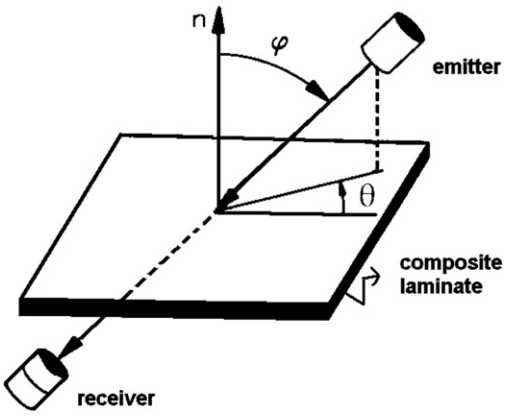

Fig. 1. The position of the transducers in a polar scan.

The position and the characteristics of these 'dark regions' are determined by the physical parameters of the plate, such as the thickness of the layers, the density and the stiffness coefficients. The damping will only influence amplitude characteristics of the registered patterns and not the exact positions of those patterns. Ultrasonic polar scans form therefore an excellent tool for monitoring these physical properties. The interpretation of a polar scan is a difficult task. However, in the case of thick plates, the only patterns that do appear are due to bulk critical angles. For reasons of explanatory simplicity we solely focus on this case. Snell's law for critical waves is as follows

$$\sin(\varphi_{\text{crit}})|_\theta = v_l / v_{\text{crit}}(\rho, C_{ij}, \theta) \tag{13}$$

where v_l is the plane wave velocity in the liquid and v_{crit} is the velocity of the critical bulk wave.

If a certain contour in one direction is wider than in other directions, it means that the velocity in the 'wider' direction is lower than in the other direction. For example the velocities of quasi longitudinal waves (corresponding to the inner contour of a polar scan) traveling along the in-plane axes of orthotropy are given by $\sqrt{C_{11}/\rho}$ and $\sqrt{C_{22}/\rho}$, respectively.

Hence, regarding Eq. (13), the directions of highest stiffness produce the smallest critical angles for quasi longitudinal waves. Even though the contours of polar scans for thin

Table 1
Properties of one layer of carbon/epoxy unidirectional fiber reinforced composites

Parameter	Value
ρ [kg/m^3]	1525
E_{11} [MPa]	$119{,}130 \times (1 - 0.0025i)$
E_{22} [MPa]	$8850 \times (1 - 0.03i)$
E_{33} [MPa]	$10{,}000 \times (1 - 0.03i)$
ν_{23}	$0.475 \times (1 - 0.015i)$
ν_{13}	$0.275 \times (1 - 0.01i)$
ν_{12}	$0.306 \times (1 - 0.01i)$
G_{23} [MPa]	$3000 \times (1 - 0.05i)$
G_{13} [MPa]	$5000 \times (1 - 0.02i)$
G_{12} [MPa]	$5500 \times (1 - 0.03i)$

plates are much more difficult to interpret, the basic idea remains unchanged.

6. Numerical examples

In a preliminary stage, we have verified our simulations for simple anisotropy. For the isotropic case for instance, we found, in agreement with the fact that every direction is acoustically the same, circular patterns with a radius corresponding to the critical angles. Our results for orthotropic media can be found in previous works.

To study ultrasonic polar scans for other types of symmetry, first of all, we consider polar scans simulated for a 1 mm thick fiber reinforced plate and an ultrasonic sound frequency of 5 MHz. For multi-layered systems, we consider layers of equal thickness. Then, in the case of composites, these calculations are performed using realistic values for the materials properties. This involves the presence of damping and is determined by means of complex valued stiffness elements [35–41].

Simulations of ultrasonic polar scans are not only developed for orthotropic materials, such as fiber reinforced composites, but also for crystals having any possible symmetry. Therefore, in what follows, some examples are shown for different kinds of crystals, having different orientations and also for the invented case of layered crystals. Depending on the considered anisotropy, specific symmetry relations hold. They can be found in numerous works, e.g., the book by Nayfeh [30].

The rotation tensor $[Q_{ij}]$ is given by

$$[Q_{ij}] = \begin{bmatrix} 1 & 0 & 0 \\ 0 & C_\alpha & S_\alpha \\ 0 & -S_\alpha & C_\alpha \end{bmatrix} \times \begin{bmatrix} C_\beta & 0 & S_\beta \\ 0 & 1 & 0 \\ -S_\beta & 0 & C_\beta \end{bmatrix} \times \begin{bmatrix} C_\gamma & S_\gamma & 0 \\ -S_\gamma & C_\gamma & 0 \\ 0 & 0 & 1 \end{bmatrix} \tag{14}$$

in which $C_\xi = \cos\xi$ and $S_\xi = \sin\xi$.

Each layer is characterized by physical parameters listed in Table 1. Figs. 2 and 3 represent the numerical simulations of ultrasonic polar scans on a double layered carbon/epoxy fiber reinforced composite with the top layer consisting of fibers in the 0° direction and the bottom layer built up by fibers in the 90° direction. We have considered 4

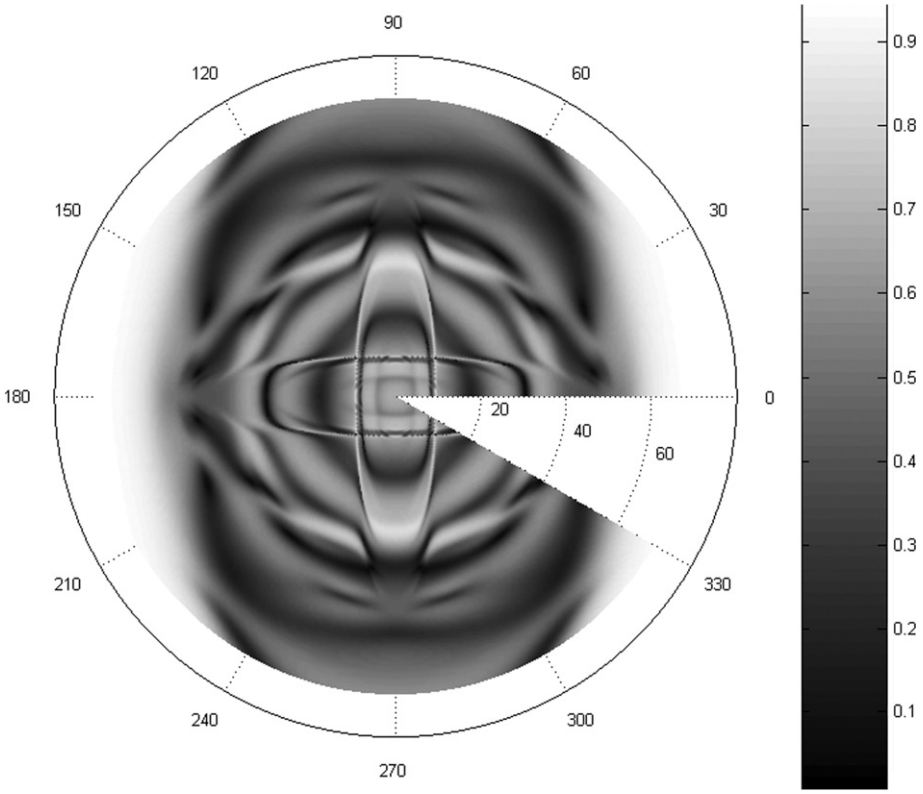

Fig. 2. Ultrasonic polar scan (harmonic, in reflection) of a double layered (0°/90°) cross-ply laminate.

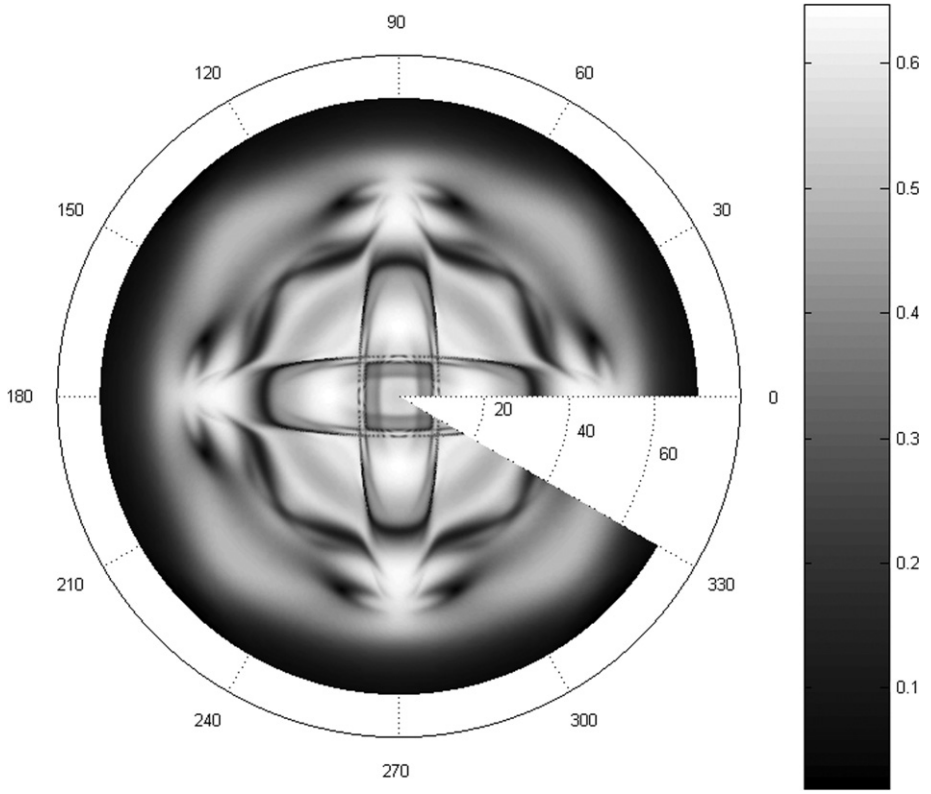

Fig. 3. Ultrasonic polar scan (harmonic, in transmission) of a double layered (0°/90°) cross-ply laminate.

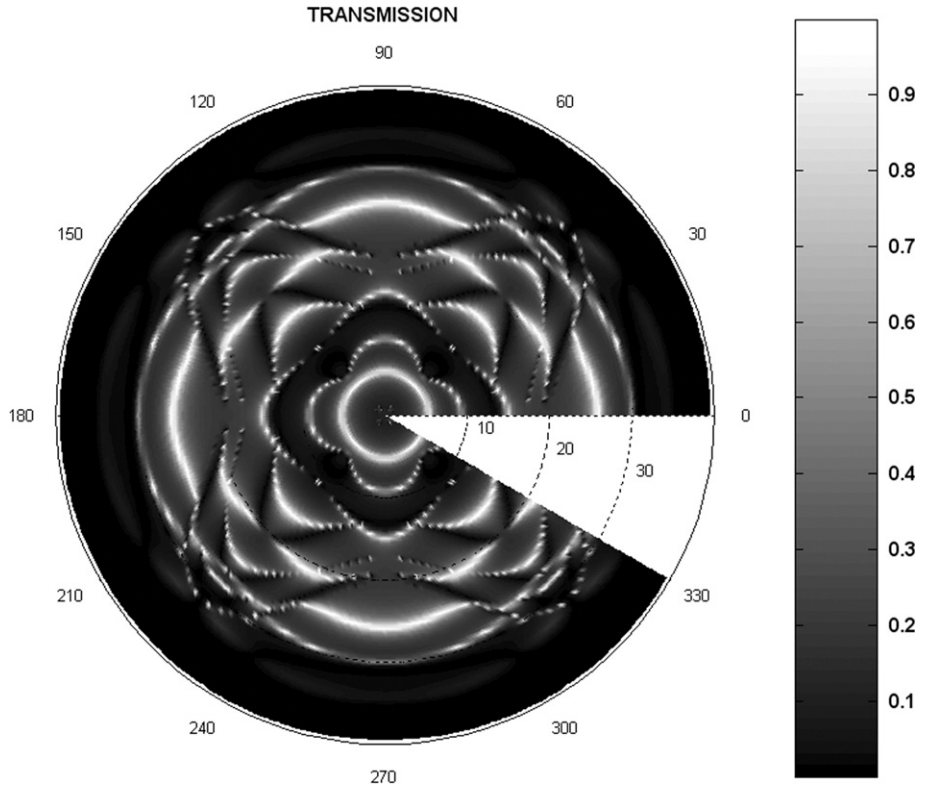

Fig. 4. Simulated polar scan in transmission for a 3 mm thick Z-cut barium titanate plate at 2 MHz.

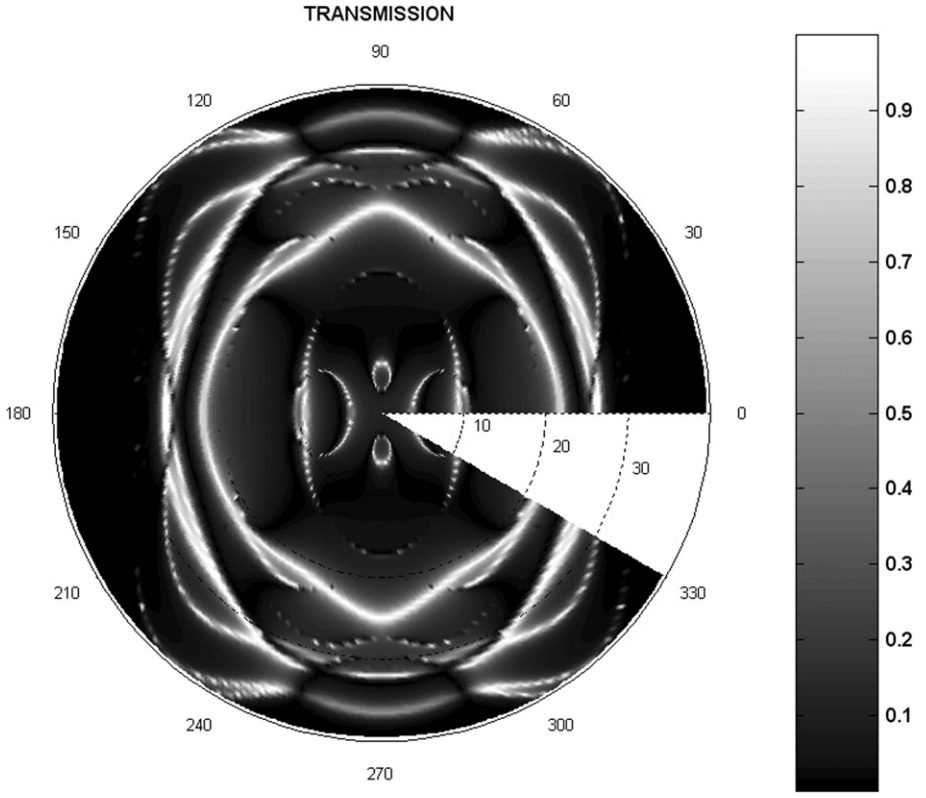

Fig. 5. Simulated polar scan in transmission for a 3 mm thick Y-cut barium titanate plate at 2 MHz.

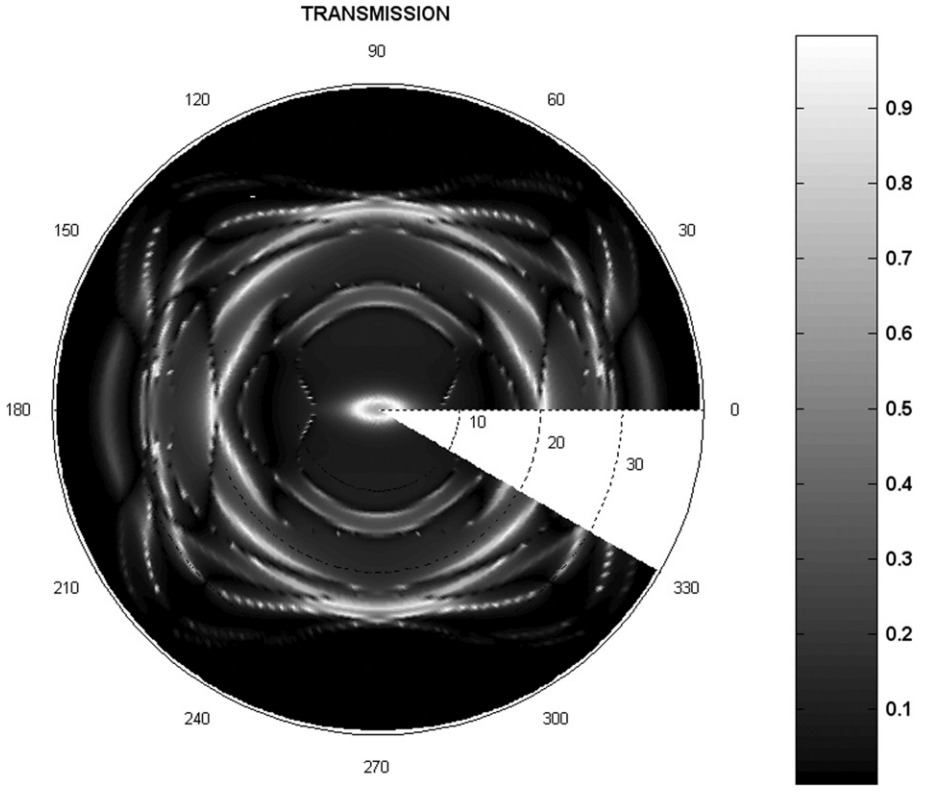

Fig. 6. Simulated polar scan in transmission for a 3 mm thick X-cut layered plate at 2 MHz.

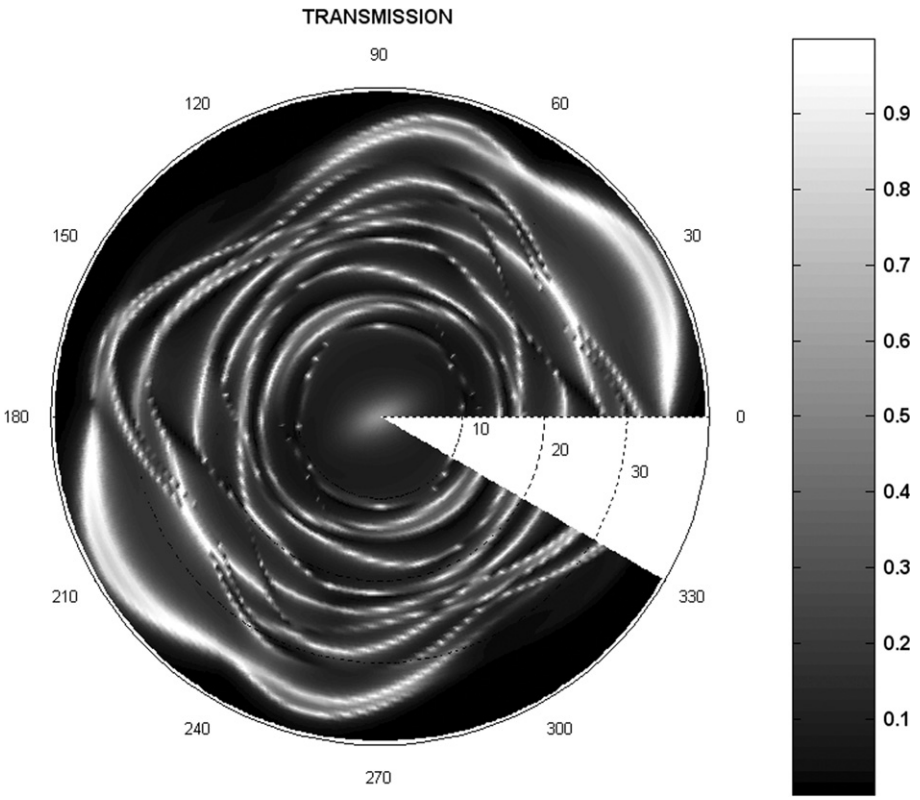

Fig. 7. Simulated polar scan in transmission for a 3 mm thick 'arbitrary'-cut layered plate at 2 MHz.

orientations, of which 3 are labeled as X-cut, Y-cut or Z-cut and the 4th is labeled as 'arbitrary':

orientation	α	β	γ
X-cut	0	$\pi/2$	0
Y-cut	$\pi/2$	0	0
Z-cut	0	0	0
'arbitrary'	$\pi/4$	$\pi/4$	$\pi/4$

(15)

We consider tetragonal 4 mm crystal material (Barium Titanate, $BaTiO_3$) and also cubic $\bar{4}3\,m$ crystal material (Gallium Arsenide, GaAs). For simplicity, we neglect piezoelectricity. The density of Barium Titanate is 6020 kgm^{-3}. The elastic constants [$\times 10^{10}$ N/m^2] are

$$C_{11} = 27.5 \quad C_{12} = 17.9 \quad C_{13} = 15.1$$
$$C_{33} = 16.5 \quad C_{44} = 5.43 \quad C_{66} = 11.3 \tag{16}$$

with

$$C_{14} = C_{15} = C_{16} = C_{24} = C_{25} = C_{26} = C_{34} = C_{35} = C_{36} = 0;$$
$$C_{45} = C_{46} = C_{56} = 0;$$
$$C_{22} = C_{11}; \quad C_{23} = C_{13}; \quad C_{55} = C_{44} \tag{17}$$

The density of Gallium Arsenide is 5307 kgm^{-3}. The elastic constants [$\times 10^{10}$ N/m^2] are

$$C_{11} = 11.88 \quad C_{12} = 5.38 \quad C_{44} = 5.94 \tag{18}$$

with

$$C_{14} = C_{15} = C_{16} = C_{24} = C_{25} = C_{26} = C_{34} = C_{35} = C_{36} = 0;$$
$$C_{45} = C_{46} = C_{56} = 0;$$
$$C_{13} = C_{12}; \quad C_{22} = C_{11}; \quad C_{23} = C_{12};$$
$$C_{33} = C_{11}; \quad C_{55} = C_{44}; \quad C_{66} = C_{44} \tag{19}$$

The crystals are immersed in water (density: 1000 kgm^{-3}, sound wave velocity: 1480 m/s).

Fig. 4 shows the simulated harmonic polar scan in transmission of a 3 mm thick Z-cut Barium Titanate crystal.

As it is known from simpler calculations for composite plates [20], the patterns are mainly due to quasi Lamb waves and are determined by the symmetry properties of the crystal and by the physical properties, such as (thickness x frequency), density and elastic constants.

Figs. 4 and 5 show the harmonic polar scans in transmission for different considered crystals and considered orientations.

Figs. 6 and 7 show similar polar scans, but now for a layered system. The system consists of two layers of equal thickness. The total thickness is again 3 mm. The orientation of both layers is equal. The examples are given for Gallium Arsenide as upper layer and Barium Titanate as lower layer. The frequency is again 2 MHz.

7. Conclusions

It is shown how numerical simulations of polar scans are performed, starting from simple principles of mechanics

and wave motion. The theoretical model has been developed for multi-layered composites and to crystals of any anisotropy. These numerical simulations, may become a means of characterizing the stiffness of anisotropic plates.

References

[1] V.T. Buchwald, A. Davis, Surface waves in anisotropic elastic media, Nature 191 (1961) 899–900.

[2] D.E. Chimenti, S.I. Rokhlin, Relationship between leaky Lamb modes and reflection coefficient zeroes for a fluid-coupled elastic layer, J. Acoust. Soc. Am. 88 (3) (1990) 1603–1611.

[3] V.T. Buchwald, Rayleigh waves in anisotropic media, Quart. J. Mech. Appl. math. XIV (9) (1961) 461–469.

[4] T.C. Lim, M.J.P. Musgrave, Stoneley waves in anisotropic media, Nature 225 (1970) 372.

[5] A.H. Nayfeh, D.E. Chimenti, Propagation of guided waves in fluid-coupled plates of fiber-reinforced composite, J. Acoust. Soc. Am. 83 (10) (1988) 1736–1743.

[6] V. Dayal, V.K. Kinra, Leaky Lamb waves in an anisotropic plate I: an exact solution and experiments, J. Acoust. Soc. Am. 85 (11) (1989) 2268–2276.

[7] D.E. Chimenti, R.W. Martin, Nondestructive evaluation of composite laminates by leaky Lamb waves, Ultrasonics 29 (1991) 13–21.

[8] T.C.T. Ting, D.M. Barnett, Classifications of surface waves in anisotropic elastic materials, Wave Motion 26 (1997) 207–218.

[9] M. Castaings, B. Hosten, The use of electrostatic, ultrasonic, air-coupled transducers to generate and receive Lamb waves in anisotropic, viscoelastic plates, Ultrasonics 36 (1998) 361–365.

[10] E. Moreno, P. Acevedo, Thickness measurement in composite materials using Lamb waves, Ultrasonics 35 (1998) 581–586.

[11] H. Jeong, D.K. Hsu, Experimental analysis of porosity-induced ultrasonic attenuation and velocity change in carbon composites, Ultrasonics 33 (3) (1995) 195–203.

[12] H. Jeong, Multiple NDE techniques for the measurement of constituent volume fractions in metal matrix composites, Res. Nondestruct. Eval. 9 (1997) 41–57.

[13] W. Zou, S. Holland, K.Y. Kim, W. Sachse, Wideband high-frequency line-focus PVDF transducer for materials characterization, Ultrasonics 41 (3) (2003) 157–161.

[14] M. Ben Amor, M.H. Ben Ghozlen, P. Lanceleur, Modelling of elastic waves generated at the interface between anisotropic media, Acta Acust. United Ac. 89 (9) (2003) 625–631.

[15] W.H.M. Van Dreumel, J.L. Speijer, Nondestructive composite laminate characterization by means of ultrasonic polar scan, Mater. Eval. 39 (15) (1981) 922–925.

[16] J. Degrieck , D. Van Leeuwen, Simulatie van een Ultrasone Polaire Scan van een Orthotrope Plaat, in: Proceedings of the 3rd Belgian National Congress on Theoretical and Applied Mechanics, Belgium: Liege University, 1994, pp. 39–42 (in Dutch).

[17] J. Degrieck, Some possibilities of nondestructive characterization of composite plates by means of ultrasonic polar scans, in: D. Van Hemelrijck, A.A. Anastassopoulos (Eds.), Non Destructive Testing, Balkema, Rotterdam, 1996, pp. 225–236.

[18] N.F. Declercq, J. Degrieck, O. Leroy, Characterization of Layered Orthotropic Materials Using Ultrasonic Polar Scans, in: Proceedings of the 2nd FTW PhD symposium, Ghent University:Belgium, 2001.

[19] N.F. Declercq, J. Degrieck, O. Leroy, Numerical simulations of ultrasonic polar scans on fiber reinforced composites, in: Proceedings of the 29 Deutsche Jahrestagung für Akustik DAGA 2003, 18–20 March 2003, Aachen, Germany, 2003.

[20] N.F. Declercq, J. Degrieck, O. Leroy, Numerical simulations of ultrasonic polar scans, in: D. Van Hemelrijck, A.A. Anastasopoulos, N.E. Melanitis (Eds.), Emerging Technologies in Nondestructive Testing, Swets & Zeitlinger, Lisse, 2004, pp. 75–80.

[21] N.F. Declercq, J. Degrieck, O. Leroy, On the influence of fatigue on ultrasonic polar scans of fiber reinforced composites, Ultrasonics 42 (2004) 173–177.

[22] L. Wang, S.I. Rokhlin, Ultrasonic wave interaction with multidirectional composites: modeling and experiment, J. Acoust. Soc. Am. 114 (10) (2003) 2582–2595.

[23] B. Hosten, M. Castaings, Surface impedance matrices to model the propagation in multilayered media, Ultrasonics 41 (12) (2003) 501–507.

[24] C. Potel, P. Gatignol, J.F. de Belleval, Energetic criterion for the radiation of Floquet waves in infinite anisotropic periodically multilayered media, Acta Acust. United Ac. 87 (3) (2001) 340–351.

[25] A.H. Naefeh, Wave propagation in layered anisotropic media with applications to composites, North Holland Series in Applied Mathematics and Mechanics (1995).

[26] M. Deschamps, B. Hosten, The effects of viscoelasticiy on the reflection and transmission of ultrasonic waves by an orthotropic plate, J. Acoust. Soc. Am. 91 (9) (1992) 2007–2015.

[27] B. Hosten, M. Castaings, Transfer matrix of multilayerd absorbing and anisotropic media measurements and simulations of ultrasonic wave propagation through composite materials, J. Acoust. Soc. Am. 94 (3) (1993) 1488–1495.

[28] K.Y. Kim, W. Zou, W. Sachse, Wave propagation in a wavy fiber-epoxy composite material: theory and experiment, J. Acoust. Soc. Am. 103 (10) (1998) 2296–2301.

[29] X.R. Lu, K.Y. Kim, W. Sachse, In situ determination of elastic stiffness constants of thick composites, Compos. Sci. Technol. 12 (1997) 753–762.

[30] M. Pluta, M. Schubert, J. Jahny, W. Grill, Angular spectrum approach for the computation of group and phase velocity surfaces of acoustic waves in anisotropic materials, Ultrasonics 38 (1–8) (2000) 232–236.

[31] V. Bucur, P. Lanceleur, B. Roge, Acoustic properties of wood in tridimensional representation of slowness surfaces, Ultrasonics 40 (1–8) (2002) 537–541.

[32] V. Bucur, Techniques for high resolution imaging of wood structure: a review, Meas. Sci. Technol. 14 (17) (2003) R91–R98.

[33] P. Lanceleur, J.F. de Belleval, N. Mercier, Synthetic tridimensional representation of slowness surfaces of anisotropic materials, Acta Acust. United Ac. 84 (11) (1998) 1047–1054.

[34] W. Maysenholder, Sound transmission through periodically inhomogeneous anisotropic thin plates: generalizations of Cremer's thin plate theory, Acta Acust. United Ac. 84 (9) (1998) 668–680.

[35] J.M. Carcione, F. Cavallini, K. Helbig, Anisotropic attenuation and material symmetry, Acta Acust. United Ac. 84 (3) (1998) 495–502.

[36] J.D. Achenbach, Wave Propagation in Elastic Solids, North Holland, Elsevier Science, Amsterdam, 1975.

[37] M.L. Dunn, Viscoelastic damping of particle and fiber reinforced composite materials, J. Acoust. Soc. Am. 98 (11) (1995) 3360–3374.

[38] S. Baudouin, B. Hosten, Immersion ultrasonic method to measure elastic constants and anisotropic attenuation in polymer-matrix and fiber-reinforced composite materials, Ultrasonics 34 (1996) 379–382.

[39] B. Vandenbossche, R.D. Kriz, T. Oshima, Stress-wave displacement polarizations and attenuation in unidirectional composites: theory and experiment, Res. Nondestruct. Eval. 8 (1996) 101–123.

[40] Kendall R. Waters, Michael S. Hughes, Joel Mobley, Gary H. Brandenburger, James G. Miller, On the applicability of Kramers-Krönig relations for ultrasonic attenuation obeying a frequency power law, J. Acoust. Soc. Am. 108 (2) (2000) 556–563.

[41] E. Moreno, P. Acevedo, M. Castillo, Thickness measurement in composite materials using Lamb waves viscoelastic effects, Ultrasonics 37 (2000) 595–599.